Spin Crossover of Spiro-Biphenalenyl Neutral Radical Molecular Conductors

Jingsong Huang, and Miklos Kertesz

More About This Article

Additional resources and features associated with this article are available within the HTML version:

- Supporting Information
- Links to the 4 articles that cite this article, as of the time of this article download
- Access to high resolution figures
- Links to articles and content related to this article
- Copyright permission to reproduce figures and/or text from this article

View the Full Text HTML

Spin Crossover of Spiro-Biphenalenyl Neutral Radical Molecular Conductors

Jingsong Huang and Miklos Kertesz*

Chemistry Department, Georgetown University, 37th & O Street, Washington, D.C. 20057

Received August 20, 2003; E-mail: kertesz@georgetown.edu

Spiro-biphenalenyl neutral radical organic materials exhibit bistability in three physical channels: optical, electrical, and magnetic.[1] Conductivities change surprisingly by 2 orders of magnitude for the ethyl (**1**)- and butyl (**2**)-substituted material at the phase transition, the temperature of which depends on the substituents.[2] The spiroconjugated neutral radicals are challenging theoretically because the two kinds of $\pi-\pi$ splittings, the intramolecular spiroconjugation and the intermolecular $\pi-\pi$ stacking interactions,[3] lead to a subtle high-spin (HS) low-spin (LS) competition. Dimerization is present in **1** and **2** but not in **3**,[1,2,4] leading to various intermolecular $\pi-\pi$ splittings. Dimerization, an accompanying spin crossover, and a change in the energy gap (E_g) due to change in occupancy are the central subjects of this work.

1, R=Et ; 2, R=Bu ; 3, R=Hx
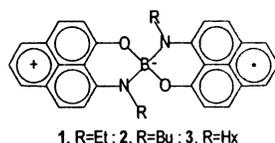
In Figure 1, we show the development of the energy bands from the half monomer of the spiroconjugated molecule. We focus only on the orbitals shown, because the other orbitals are lower or higher than these orbitals by at least 1 eV.[2] Spiroconjugation at the central boron atom leads to an intramolecular $\pi-\pi$ energy level splitting, E_{g1}, in the order of 0.5 eV. In the case of a neutral radical, the lower level is the singly occupied molecular orbital, SOMO.[4] Upon dimer formation, these two monomer levels split into four levels because of $\pi-\pi$ intermolecular interactions. In the figure, the $\pi-\pi$ overlap is shown for the first and the fourth dimer levels. It appears that this packing has the largest number of overlaps between the larger lobes. The energy level splittings are sensitive to the separation, d,[5] between the two overlapping phenalenyl rings in the dimer. According to our DFT calculations, this splitting, E_{g2}, is ca. 0.14 eV for the high-temperature polymorph and is ca. 0.2 eV for the low-temperature polymorph. For the dimer, the two unpaired electrons coming from the two SOMOs occupy the lowest dimer orbital, leading to intermolecular covalent-type bonding,[6] which is partially responsible for the closer separation than the sum of the van der Waals radii. At higher temperatures, the next dimer orbital becomes thermally populated, reducing the effect of the intermolecular $\pi-\pi$ bonding. As a result, the intermolecular separation increases up to the van der Waals value. (The d−temperature relationship is shown in Figure 2.)

In the unit cell, there are two sets of dimers, further splitting the four dimer MOs into eight bands, leading to two filled bands and six empty ones in the LS state case. Because E_{g2} is sensitive to the intermolecular separation, it is possible that the spin state preference for the dimer is HS for the high-temperature polymorph, while it is LS for the low-temperature one. When this idea is applied to solid state, the question becomes whether the observed gap corresponds to E_{g3} (LS) or E_{g4} (HS).
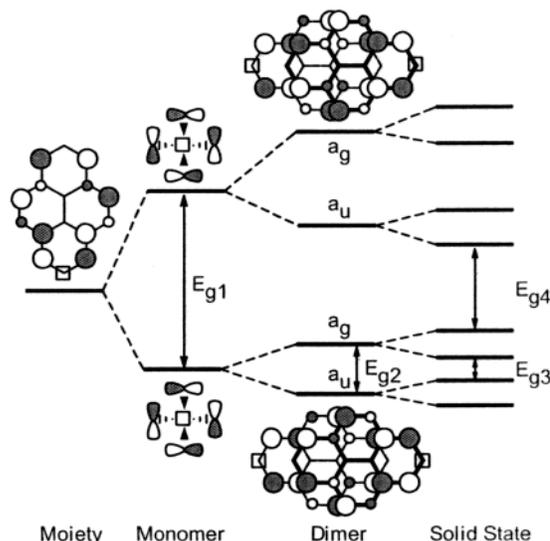
Figure 1. Band structure development of spiro-biphenalenyl neutral radical organic solid from the orbitals of the half monomer. Boron atoms (□) are at the center of spiroconjugation. Substituents are omitted; the top view of the dimer orbitals shows (for side view, see Supporting Information) the $\pi-\pi$ overlap with a small offset for clarity for the first and the fourth dimer levels. The second dimer orbital is similar to the fourth one, and the third is similar to the first one, except for the spiroconjugation interaction. E_{g1}, E_{g2}, E_{g3}, and E_{g4} are energy gaps discussed in the text.
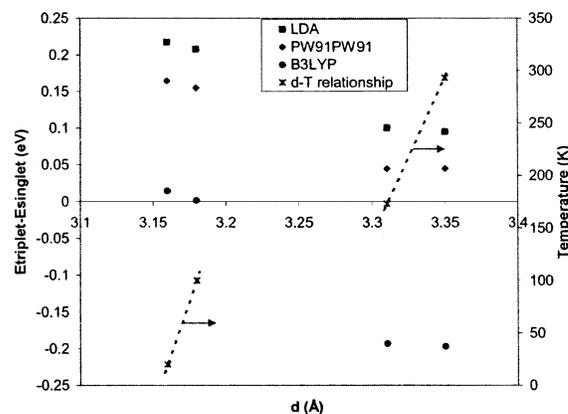
Figure 2. Spin state preference of the dimer of **1** calculated at three different theoretical levels as discussed in the text. Dimer geometries are taken from crystal structures; the temperatures at which the four intermolecular separations were obtained[2] are indicated on the right axis.

We first performed total energy calculations for the dimer at several levels of theory with the 6-31G* basis set.[7,8] The results are shown in Figure 2 at four different intermolecular separations corresponding to the four temperatures at which structures are available. Local density approximation (LDA)[9] and 1991 Perdew−Wang functionals (PW91PW91)[10] predict LS singlet states for all of the four structures. Becke's three parameter hybrid functional
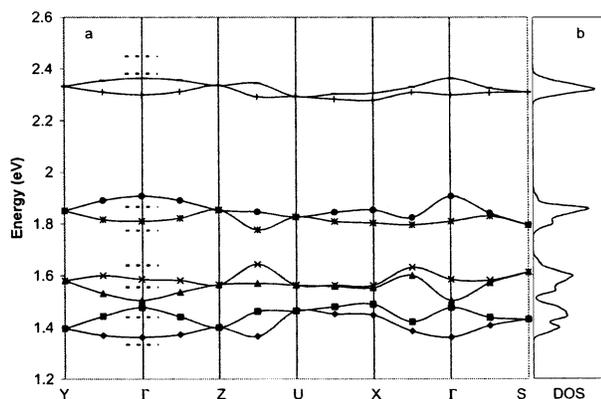
Figure 3. (a) Band structure and (b) density of states (DOS) of the 173 K structure of **1**.[16,17] Dashed horizontal bars at the Γ point correspond to energy levels from the solid-state calculation for the 100 K structure.

with Lee−Yang−Parr correlation functional (B3LYP)[11] predicts HS triplet states for the two high-temperature structures and LS singlet states for the two low-temperature structures. B3LYP has been widely used for predicting spin state preferences of molecules, yielding good agreement with post-HF correlation calculations and with experiments.[12−14] HF often overestimates the relative stability of HS states.[14,15] LDA and PW91PW91 probably underestimate the stability of triplets because of the reduced exchange terms of these levels of theory.

Solid-state calculations were done using the Vienna ab initio simulation package (VASP).[16] The band structure for the 173 K polymorph from the non spin-polarized calculation is shown in Figure 3.[17] The lowest two bands are nearly touching the next two bands, with a gap of only 0.03 eV. We also did a $1 \times 1 \times 1$ k-mesh calculation for the 100 K polymorph, and the corresponding levels are shown in Figure 3 at the Γ point by horizontal dashed bars. Accordingly, E_{g3} increases from the 0.03 eV value (173 K) to 0.12 eV (100 K) due to the increased intradimer overlap as d is decreasing from 3.31 to 3.18 Å.

On the basis of these calculations and the experiments of the Haddon group,[1,2] we present the following interpretation: above the phase transition, the lowest four bands will be singly occupied by the electrons coming from the SOMOs of the four molecules in the unit cell. This HS state is supported by the observation of one curie spin per molecule from magnetism measurements.[1,2] The experimentally observed gap should then correspond to E_{g4}. Below the phase transition temperature, only the lowest two bands will be doubly occupied corresponding to a LS state. This LS state is also supported by the quenched paramagnetism with virtually zero curie spin on each molecule.[1,2] In this case, the experimentally observed gap should correspond to E_{g3}.

For the 173 K structure, the band gap, E_{g4}, is 0.23 eV at the Γ point.[18] The IR spectrum (at 160 K) shows an onset of the electronic transition at ca. 0.22 eV.[1] A gap of 0.23 eV is also obtained for structures above the phase transition temperature from T dependence of the conductivity.[2] For the 100 K structure, E_{g3} is 0.12 eV at the Γ point. The IR spectrum (at 110 K) shows an onset of the electronic transition at ca. 0.10 eV.[1] The same value is also obtained for the structures below the phase transition temperature from conduction measurements.[2] Therefore, the calculated gaps agree with experiments.

The unusual change of conductivity at the phase transition can be understood as a consequence of two different gaps: $E_{g3} = 0.1$ eV for the low T phase, and $E_{g4} = 0.23$ eV for the high T phase. The resulting difference in the number of charge carriers around

the phase transition (between 125 and 145 K) is approximately 2 orders of magnitude according to the approximation $n = n_0 \exp(-E_g/2kT)$. The change of conductivity at the phase transition of **2**[2] can be also qualitatively understood on the basis of our calculations presented herein. This phenomenon is absent for **3**[1,4] because there is no spin crossover for this Mott−Hubbard-like insulator as reflected in the absence of dimer formation.

In summary, we have shown that for the spiro-biphenalenyl neutral radical organic conductors, a different band becomes the conduction band due to a spin crossover at the phase transition. The energy gap (E_g) increases from 0.12 eV of the low-temperature polymorph to 0.23 eV of the high-temperature polymorph because it corresponds to a different occupancy causing a change in the number of available charge carriers, explaining the change of conductivity by 2 orders of magnitude. Other properties are also consistent with this interpretation.

Supporting Information Available: Side view of dimer orbital, table of total energy differences ($\Delta E_{T−S} = E_{triplet} − E_{singlet}$), and comments to Figure 3 (PDF). This material is available free of charge via the Internet at http://pubs.acs.org.

References

(1) Itkis, M. E.; Chi, X.; Cordes, A. W.; Haddon, R. C. *Science* **2002**, *296*, 1443.
(2) Chi, X.; Itkis, M. E.; Kirschbaum, K.; Pinkerton, A. A.; Oakley, R. T.; Cordes, A. W.; Haddon, R. C. *J. Am. Chem. Soc.* **2001**, *123*, 4041.
(3) It is essential to use an appropriate level of theory and basis set to obtain reliable intermolecular level splittings, see: Huang, J.; Kertesz, M. *J. Phys. Chem. B* **2003**, *107*, in press.
(4) Chi, X.; Itkis, M. E.; Patrick, B. O.; Barclay, T. M.; Reed, R. W.; Oakley, R. T.; Cordes, A. W.; Haddon, R. C. *J. Am. Chem. Soc.* **1999**, *121*, 10395.
(5) Brédas, J. L.; Calbert, J. P.; da Silva Filho, D. A.; Cornil, J. *Proc. National Acad. Sci. U.S.A.* **2002**, *99*, 5804.
(6) (a) Brocks, G. *J. Chem. Phys.* **2000**, *112*, 5353. (b) Novoa, J. J.; Lafuente, P.; Del Sesto, R. E.; Miller, J. S. *Angew. Chem., Int. Ed.* **2001**, *40*, 2540. (c) Takano, Y.; Taniguchi, T.; Isobe, H.; Kubo, T.; Morita, Y.; Yamamoto, K.; Nakasuji, K.; Takui, T.; Yamaguchi, K. *J. Am. Chem. Soc.* **2002**, *124*, 11122.
(7) Frisch, M. J.; Trucks, G. W.; Schlegel, H. B.; Scuseria, G. E.; Robb, M. A.; Cheeseman, J. R.; Zakrzewski, V. G.; Montgomery, J. A., Jr.; Stratmann, R. E.; Burant, J. C.; Dapprich, S.; Millam, J. M.; Daniels, A. D.; Kudin, K. N.; Strain, M. C.; Farkas, O.; Tomasi, J.; Barone, V.; Cossi, M.; Cammi, R.; Mennucci, B.; Pomelli, C.; Adamo, C.; Clifford, S.; Ochterski, J.; Petersson, G. A.; Ayala, P. Y.; Cui, Q.; Morokuma, K.; Malick, D. K.; Rabuck, A. D.; Raghavachari, K.; Foresman, J. B.; Cioslowski, J.; Ortiz, J. V.; Stefanov, B. B.; Liu, G.; Liashenko, A.; Piskorz, P.; Komaromi, I.; Gomperts, R.; Martin, R. L.; Fox, D. J.; Keith, T.; Al-Laham, M. A.; Peng, C. Y.; Nanayakkara, A.; Gonzalez, C.; Challacombe, M.; Gill, P. M. W.; Johnson, B. G.; Chen, W.; Wong, M. W.; Andres, J. L.; Head-Gordon, M.; Replogle, E. S.; Pople, J. A. *Gaussian 98*, revision A.11.4; Gaussian, Inc.: Pittsburgh, PA, 2002.
(8) PQS version 2.3, Parallel Quantum Solutions, 2013 Green Acres Road, Fayetteville, AR.
(9) (a) Slater, J. C. *Quantum Theory of Molecular and Solids*; McGraw-Hill: New York, 1974; Vol. 4. (b) Vosko, S. H.; Wilk, L.; Nusair, M. *Can. J. Phys.* **1980**, *58*, 1200.
(10) Perdew, J. P.; Wang, Y. *Phys. Rev. B* **1992**, *45*, 13244.
(11) (a) Becke, A. D. *J. Chem. Phys.* **1993**, *98*, 5648. (b) Lee, C.; Yang, W.; Parr, R. G. *Phys. Rev. B* **1988**, *37*, 785.
(12) Gogonea, V.; Schleyer, P. v. R.; Schreiner, P. R. *Angew. Chem., Int. Ed.* **1998**, *37*, 1945.
(13) Ito, A.; Ino, H.; Ichiki, H.; Tanaka, K. *J. Phys. Chem. A* **2002**, *106*, 8716.
(14) Mitani, M.; Mori, H.; Takano, Y.; Yamaki, D.; Yoshioka, Y.; Yamaguchi, K. *J. Chem. Phys.* **2000**, *113*, 4035.
(15) Saito, T.; Ito, A.; Tanaka, K. *J. Phys. Chem. A* **1998**, *102*, 8021.
(16) (a) Kresse, G.; Furthmüller, J. *Phys. Rev. B* **1996**, *54*, 11169. (b) Kresse, G.; Hafner, J. *Phys. Rev. B* **1993**, *47*, 558; using PW91PW91 functionals together with Vanderbilt-type (Vanderbilt, D. *Phys. Rev. B* **1990**, *41*, 7892) ultrasoft pseudopotentials (Kresse, G.; Hafner, J. *J. Phys.: Condens. Matter* **1994**, *6*, 8245). Cutoff energy was 286.7 eV.
(17) The band structure is presented along several directions, see for example: Puschnig, P.; Ambrosch-Draxl, C. *Phys. Rev. B* **1999**, *60*, 7891.
(18) A direct gap of 0.14 eV is found along the Z−U line, but the density of states (DOS) indicates a larger peak-to-peak gap of 0.26 eV.

JA038038+